

# Remarkable Scan Rate Dependence for a Highly Constrained Dinuclear Iron(II) Spin Crossover Complex with a Wide Thermal Hysteresis Loop

Rafal Kulmaczewski,<sup>†</sup> Juan Olguin,<sup>†</sup> Jonathan A. Kitchen,<sup>†</sup> Humphrey L. C. Feltham,<sup>†</sup> Guy N. L. Jameson,<sup>†</sup> Jeffery L. Tallon,<sup>‡</sup> and Sally Brooker<sup>\*,†</sup>

<sup>†</sup>Department of Chemistry and MacDiarmid Institute for Advanced Materials and Nanotechnology, University of Otago, P.O. Box 56, Dunedin 9054, New Zealand

<sup>‡</sup>MacDiarmid Institute for Advanced Materials and Nanotechnology and Robinson Research Institute, Victoria University of Wellington, P.O. Box 31310, Lower Hutt, New Zealand

## Supporting Information

**ABSTRACT:** The abrupt [HS-HS] ↔ localized [HS-LS] spin crossovers of a new triazole-based diiron(II) complex result in a record-equaling thermal hysteresis loop width for a dinuclear complex ( $\Delta T = 22$  K by SQUID magnetometer in “settle” mode) and show a remarkable scan rate dependence of only the cooling branch, as revealed by detailed magnetic, DSC, and Mössbauer studies.

Spin crossover (SCO) occurs when a transition metal ion is switched from high spin (HS) to low spin (LS) by application of an external stimulus such as temperature, pressure, magnetic/electric field, or light irradiation.<sup>1</sup> SCO is either gradual (occurs over a wide temperature range) or abrupt (occurs within a few degrees), in which case it is termed a spin transition (ST). ST is the result of high cooperativity between spin centers, and so it can also produce thermal hysteresis; i.e., the  $T_{1/2}$  (temperature at which HS:LS = 1:1) is lower on cooling ( $T_{1/2\downarrow}$ ) than on heating ( $T_{1/2\uparrow}$ ). Hence, the compound also exhibits bistability (memory effect). From an applications point of view,<sup>2</sup> ST with a wide hysteresis loop ( $\Delta T$ ) spanning room temperature (RT) is desirable.

To date, very few complexes show really wide ( $\Delta T > 100$  K) thermal hysteresis loops that are reproducible with repeated scanning.<sup>3</sup> The widest of these are seen for monometallic complexes (Table S1):  $\Delta T \approx 140$  K for both  $[\text{Fe}^{\text{II}}(\text{bpp})_2](\text{CF}_3\text{SO}_3)_2 \cdot \text{H}_2\text{O}$ , with an asymmetric two-step ST upon heating,<sup>4</sup> and  $[\text{Co}^{\text{II}}(\text{C}_{12}\text{-terpy})_2](\text{BF}_4)_2$ , for a “reverse” ST;<sup>5</sup>  $\Delta T \approx 90$  K for  $[\text{Fe}^{\text{II}}(2\text{-pic})_3]\text{Cl}_2 \cdot \text{H}_2\text{O}$ , but only when cooled slowly.<sup>6</sup> For  $[\text{Fe}^{\text{II}}(\text{PM-PEA})_2(\text{NCS})_2]$ ,  $\Delta T$  could be expanded from 37 to 100 K by application of 2.6 kbar external pressure.<sup>7</sup> However, as noted, all of these examples are “special cases”.

To the best of our knowledge, the widest  $\Delta T$  for a structurally characterized iron(II) complex is 70 K, reported for a monometallic iron(II) complex of a Jäger-type ligand: this is also an example of the simplest type of hysteretic behavior (both STs occur abruptly and in one step). The very high cooperativity between spin centers was ascribed to a 2D network of hydrogen-bonding interactions.<sup>8</sup> The widest loops reported for any polymeric materials are of a similar magnitude,  $\Delta T \approx 60$  K for

a Kahn-type 1D polymer of a 4-amino-1,2,4-triazole,  $[\text{Fe}^{\text{II}}(\text{NH}_2\text{trz})_3](\text{NO}_3)_{1.7}(\text{BF}_4)_{0.3}$ ,<sup>2a</sup> and for a 3D polymer,  $\{\text{Fe}^{\text{II}}(\text{pz})[\text{Pt}(\text{CN})_4]\} \cdot 0.5(\text{CS}(\text{NH}_2)_2)$ .<sup>9</sup>

In dinuclear iron(II) complexes  $[\text{HS-HS}] \leftrightarrow [\text{LS-LS}]$  SCO can take place either in one step<sup>10</sup> or in two steps via a “half” SCO state, “[HS-LS]”. The “[HS-LS]” state can be either a 50:50 mixture of [HS-HS] and [LS-LS],<sup>11</sup> or a fully localized [HS-LS] state.<sup>12</sup> We are aware of only five cases of thermal hysteresis in dinuclear complexes:<sup>13</sup> four with  $\Delta T < 13$  K (Table S1)<sup>14</sup> and one which, prior to the present study, had the widest hysteresis loop reported for a dinuclear complex,  $\Delta T = 21$  K.<sup>15</sup>

Presumably the bulk of these studies were, correctly, performed with the magnetometer in “settle” mode, with small steps between temperatures and long equilibration times at each  $T$  (so the sample easily keeps up with the rate of  $T$  change);<sup>16</sup> however, unfortunately, this key fact is not always stated (Table S1). This is of concern, as these instruments can also operate in a sweep (or continuous) mode, in which case the rate of change is of course critically important. This is because thermal hysteresis can result from a lag in responding to the change in  $T$ , where the hysteresis loop will be wider at high scan speeds and narrower at low scan speeds, potentially closing ( $\Delta T \rightarrow 0$ ) as the scan speed approaches 0, providing the barrier in  $\Delta G$  between the HS and LS states in the observed  $T_{1/2\downarrow}$  to  $T_{1/2\uparrow}$  range is not too large.<sup>16</sup> This point may well be understood by experts, but actual, illustrated examples and related discussion have not appeared in key SCO reviews or books.<sup>17</sup> This, when combined with the lack of scan rate information in some papers, represents a very real potential trap for synthetic chemists entering this field. Indeed, there are surprisingly few published examples where the *scan rate dependence of hysteretic thermal (not light-induced) ST* has been investigated,<sup>6,9,18</sup> and all of these concern mononuclear or polymeric iron(II) complexes. These studies show that where the increase of the scan speed does not affect the shape of the loop, it increases  $\Delta T$ —except in a very recently reported case where decreasing the scan rate gave an increase in  $\Delta T$  (due to a kinetically controlled phase transition between two independent and stable LS phases which are related to the same HS phase).<sup>18f</sup> The general lack of scan rate dependence studies of thermal

Received: November 14, 2013

Published: January 8, 2014

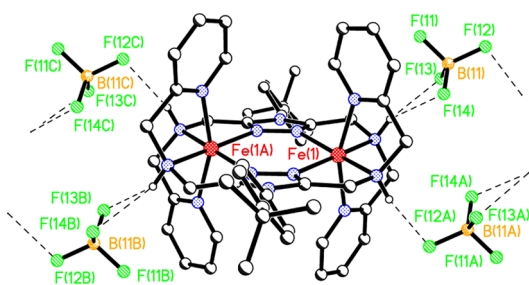


Figure 1. Perspective view of **1'** at 90 K (solvents omitted for clarity).

hysteresis represents a missed opportunity to further probe and better understand these processes.

Here we report the first detailed scan rate study on a dinuclear complex,  $[\text{Fe}^{\text{II}}_2(\text{PMPH}^{\text{tbuT}})_2](\text{BF}_4)_4 \cdot 3.5\text{H}_2\text{O}$  (**1**), which undergoes an abrupt and hysteretic thermally induced half-ST from [HS-HS] to localized [HS-LS], with one of the largest reported  $\Delta T$  values for a dinuclear complex and a remarkable rate dependence (Figure 2). The resulting scan rate vs  $T_{1/2\downarrow}$  and  $T_{1/2\uparrow}$  plot (Figure 3) is unique.

Recrystallization of the pinkish solid obtained from 1:1 reactions of  $\text{Fe}(\text{BF}_4)_2 \cdot 6\text{H}_2\text{O}$  with  $\text{PMPH}^{\text{tbuT}}$ , from 4:1 MeCN/DMF by vapor diffusion of diethyl ether, results in colorless single crystals of  $[\text{Fe}^{\text{II}}_2(\text{PMPH}^{\text{tbuT}})_2](\text{BF}_4)_4 \cdot 3\text{CH}_3\text{CN} \cdot 1/2(\text{C}_4\text{H}_{10}\text{O})$  (**1'**). Structural characterization of **1'** shows it is [HS-HS] at 91 K (av. Fe–N = 2.185 Å;  $\Sigma = 118^\circ$ ; Figures S1, and S2, Tables S3–S5). Magnetic susceptibility measurements from 300 to 2 K confirm that **1'** is not SCO active, i.e., this solvatomorph remains [HS-HS] (Figure S3). In contrast, filtration and air drying of the crystals reproducibly gives off-white **1** (for details see Supporting Information), which magnetic susceptibility measurements reveal undergoes a thermally induced, reversible, half ST from [HS-HS] to [HS-LS] (Figure S4). Subsequently, the magnetic susceptibility study was rerun in “sweep” mode with five consecutive cycles run at scan speeds of 0.2–10  $\text{K min}^{-1}$ , across the temperature window of the hysteresis loop, from 240 to 160 K (Figure 2).

At all scan rates, abrupt and hysteretic ST between [HS-HS] and [LS-HS] is observed, in both the cooling and heating modes. At 240 K, the  $\chi T$  value,  $7.2 \text{ cm}^3 \text{ K mol}^{-1}$ , is consistent with both iron(II) being HS, whereas at 160 K,  $\chi T = 3.9 \text{ cm}^3 \text{ K mol}^{-1}$ , consistent with a half SCO [HS-LS] state.<sup>12a</sup> At 10  $\text{K min}^{-1}$ , on cooling the half-ST is observed at  $T_{1/2\downarrow} = 175.4 \text{ K}$ , and on heating  $T_{1/2\uparrow} = 216.6 \text{ K}$ , giving the widest hysteresis loop reported to date for dinuclear complex, albeit a kinetic one, of  $\Delta T = 41 \text{ K}$ . The scan rate study (Figure 2) reveals that the loop width is scan rate dependent, ranging from 22 to 41 K for sweep rates of 0.2–10  $\text{K min}^{-1}$  (Table S7). Surprisingly, though, the heating branch  $T_{1/2\uparrow}$  is practically invariant (varying by just 1.7 K, Table S7, Figure 3), whereas the cooling branch  $T_{1/2\downarrow}$  values are affected by the scan speed (varying by 18.5 K, as might be expected). Hence, the hysteresis loop narrows only “at one end” (Figures 3 and S5).

To determine the “real” curve for the cooling branch of the hysteresis, the sample was rapidly cooled (at 10  $\text{K min}^{-1}$ ) to  $T = 190, 195, \text{ or } 200 \text{ K}$  (within the loop), and in each case  $T$  held constant while  $\chi$  was measured over time,  $\chi_{(t \rightarrow \infty)}$ , to give relaxation rate curves (Figures S6–S8) from which a 0  $\text{K min}^{-1}$  scan rate cooling branch was estimated (Figure 2, ■ and black line). The resulting  $\Delta T = 21 \text{ K}$  loop is, within experimental error, the same as that observed at the slowest sweep rate (0.2  $\text{K min}^{-1}$ ;  $\Delta T = 22 \text{ K}$ ) and that obtained by plotting  $T_{1/2}$  vs scan rate and by estimating by linear extrapolation to zero scan rate (Figure S9,

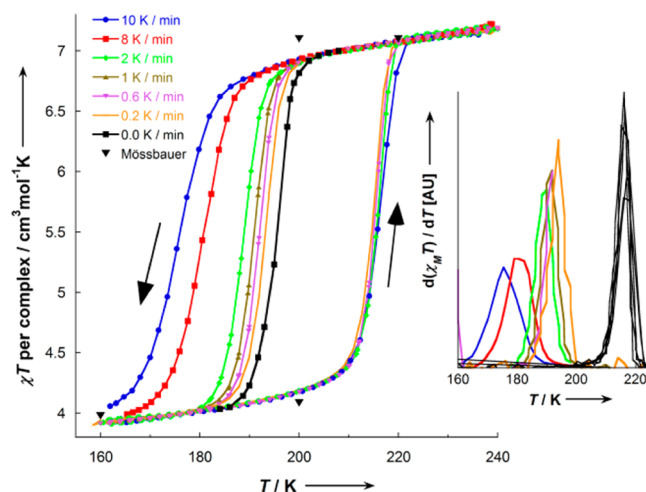


Figure 2. Scan rate study (0.2–10  $\text{K min}^{-1}$ ) of  $\chi T$  vs  $T$  for **1**, plus the infinitely slow scan rate curve estimated from the relaxation studies (■ and black line; see Supporting Information) and the values calculated from the Mössbauer data (▼) assuming one HS Fe(II) ion is  $3.55 \text{ cm}^3 \text{ mol}^{-1} \text{ K}^{-1}$ . Inset:  $d(\chi T)/dT$  vs  $T$  plot used to determine  $T_{1/2}$  values.

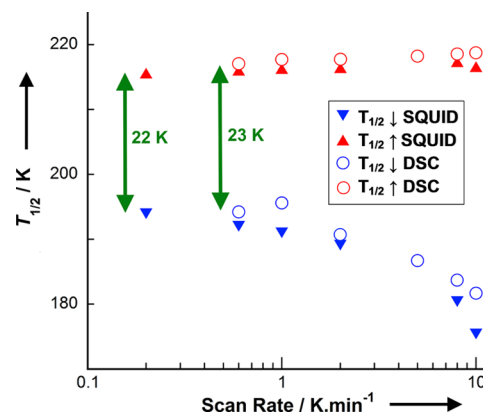
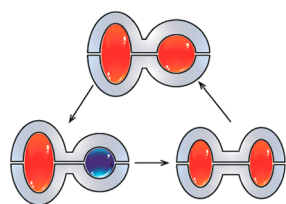


Figure 3. Semi-log plot of the scan rate dependence of  $T_{1/2\downarrow}$  and  $T_{1/2\uparrow}$  values for **1**, determined from magnetic (triangles) and DSC (circles) measurements.

$\Delta T = 23 \text{ K}$ ), and equals the record set for dinuclear complexes by Weber et al.<sup>15</sup>

That the loop is not observed to close ( $\Delta T = 0$ ) as the scan speed nears 0 (as might be expected) implies that, at the observed  $T_{1/2\downarrow}$  to  $T_{1/2\uparrow}$  range for **1**, the barrier in  $\Delta G$  between the [HS-HS] and [HS-LS] states is significant,<sup>16</sup> resulting in a long lifetime for the metastable state (perhaps even  $>24 \text{ h}$ , Figure S9), which is a good step toward the lifetimes of  $>10 \text{ years}$  that will likely be needed in device applications. Interestingly the relaxation curves (Figures S6–S8) obtained for the cooling branch do not obey first order kinetics, rather they reveal that this process has two distinct relaxation constants, consistent with another state being involved in this transformation. We propose that before thermally induced [HS-HS]  $\rightarrow$  [HS-LS] ST can occur, the HS iron(II) centers first adopt a vibrationally excited [HS-HS] state in which one of them is less distorted (and can subsequently switch to LS) while the other one is more distorted, due to the highly constrained nature of the  $\text{PMPH}^{\text{tbuT}}$  ligand, and it remains HS (Figure 4).

In this and other dinuclear complexes of such PMRT ligands, all 12 donors to the two Fe(II) centers come from just two ligands that also doubly bridge the metal centers, resulting in a highly constrained environment (Table S5).<sup>12a,19</sup> This is likely



**Figure 4.** Generalized view of a possible explanation for the unusual kinetic data obtained on **1**. Two bis-terdentate PMPH<sup>tbuT</sup> ligands in gray; iron ions in blue (LS) and red (HS; circle vs small ellipse vs large ellipse show increasing distortion).

also why the [LS-LS] state has not been observed for any PMRT complex. Unlike the cooling branch, the heating branch, [HS-LS] → [HS-HS] ST, is not scan-rate dependent, probably because converting the LS center to HS releases the ligand-strain inherent in this PMRT ligand, conforming to the more closely octahedral geometry required for LS than for HS iron(II) (Figure 4;  $\Sigma(\text{LS}) = 65\text{--}70^\circ$ ;  $\Sigma(\text{HS}) = 88\text{--}118^\circ$  in [HS-HS] vs  $123\text{--}133^\circ$  in [HS-LS]).<sup>12a,19</sup>

Differential scanning calorimetry (DSC) experiments conducted on **1**, with the same scan speeds as for the magnetic measurements, confirm the presence of thermal hysteresis that is scan rate dependent only in the cooling branch (Figures 3, 5, and S15, Tables S7 and S8). The exothermic/endothemic processes observed on the cooling/warming paths, respectively, peaked at similar temperatures to those obtained from the magnetic data and  $T_{1/2\uparrow}$  was again independent of scan speed (Figures 3 and 5, Table S7).

The thermodynamic parameters were calculated from the DSC data in two ways, (a) using the DSC integration software (Figures S10 and S11) and (b) calculating the excess heat capacities  $\Delta C_p$  (Figures 5, S12–S14), and were in good agreement (Table S8). Interestingly, again the heating mode parameters,  $\Delta H_\uparrow$  ( $12.2\text{--}13.2\text{ kJ mol}^{-1}$ ) and  $\Delta S_\uparrow$  ( $55.6\text{--}60.8\text{ J K}^{-1}\text{ mol}^{-1}$ ), remain relatively constant, regardless of scan speed ( $10\text{--}0.6\text{ K min}^{-1}$ ), whereas the cooling mode parameters,  $\Delta H_\downarrow$  ( $9.8\text{--}18.3\text{ kJ mol}^{-1}$ ) and  $\Delta S_\downarrow$  ( $54.2\text{--}94.0\text{ J K}^{-1}\text{ mol}^{-1}$ ), are scan rate dependent, further supporting our proposal that the [HS-HS] → [HS-LS] ST is more complex than the [HS-LS] → [HS-HS] ST (Figure 4). These values are as expected for iron(II) systems<sup>1</sup> and are close to the overall values determined for the two-step non-hysteretic SCO seen for the dinuclear complex  $[\{\text{Fe}(\text{bt})(\text{NCS})_2\}_2(\text{bpym})]$  ( $\Delta H = 13\text{ kJ mol}^{-1}$  and  $\Delta S = 82\text{ J K}^{-1}\text{ mol}^{-1}$ ).<sup>20</sup> As usual, the entropy values are much larger than can be attributed to the change in spin multiplicity alone ( $\Delta S = R \ln(2\Delta S_{\text{mult}} + 1) = 13.4\text{ J mol}^{-1}\text{ K}^{-1}$ ), consistent with a large vibrational entropy component upon ST.<sup>1,21</sup>

The abruptness of the STs observed for **1** was further investigated by analysis of the DSC data using the Sorai and Seki phenomenological domain model (eq S2 and Figures S20 and S21),<sup>21,22</sup> which calculates the number of interacting spin centers  $n$  per domain (higher  $n$  = more cooperative ST).<sup>16</sup> The experimental  $\Delta C_{p\uparrow}$  and  $\Delta C_{p\downarrow}$  values vs  $T$  were simulated at each scan rate, giving  $n_\uparrow \approx 28$  and  $n_\downarrow = 10\text{--}12$ , regardless of scan rate (Figure S21). This indicates that the [HS-LS] → [HS-HS] ST is about twice as cooperative (as twice the number of centers interact) as the [HS-HS] → [HS-LS] ST. While this model does not account for hysteresis, when the domain sizes in the cooling and warming modes differ significantly, as it is the case here, hysteresis may be expected.<sup>16,18c</sup>

The Slichter–Drickamer model (eq S3)<sup>23</sup> was employed to model the hysteretic behavior,<sup>18c</sup> with cooperativity indicated by

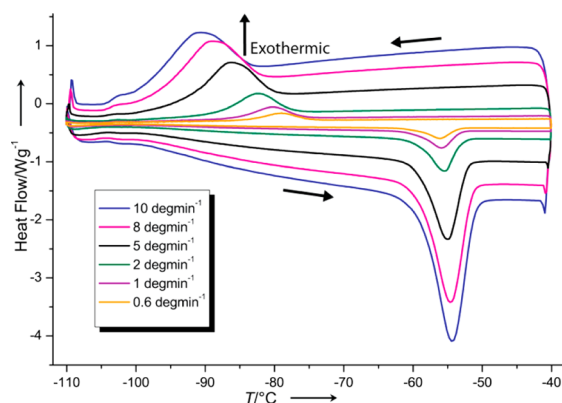


**Figure 5.** Scan rate ( $0.6\text{--}10\text{ K min}^{-1}$ ) DSC study for **1**, showing the exo- and endothermic transitions seen on cooling and heating.

the mean-field interaction term  $\Gamma$  (hysteretic systems should have  $\Gamma > 2RT_c$  where  $T_c = 1/2(T_{1/2\uparrow} + T_{1/2\downarrow})$ ). For each scan speed, the  $T_c$  and HS molar fractions ( $\gamma_{\text{HS}}$ ) were calculated from the magnetic data, then  $\Delta H = 1/2(\Delta H_\uparrow + \Delta H_\downarrow)$  was calculated from the DSC measurements by integration of  $\Delta C_p$ , followed by (using  $T_c$  and  $\Delta H$ )  $\Delta S$  (Table S10). All of the experimental hysteresis curves are very well reproduced with  $\Gamma = 4.9\text{--}5.1$ , regardless of scan speed (Figure S23). So  $\Gamma$  ( $\sim 5\text{ kJ mol}^{-1}$ ), and hence the extent of the cooperative interaction, is practically invariant over these scan rates and is greater than  $2RT_c$  ( $\sim 3.3\text{ kJ mol}^{-1}$ ), consistent with the observed hysteresis.

The variable-temperature <sup>57</sup>Fe Mössbauer study of **1** (Figure S16, Table S9) confirms (a) the presence of the hysteresis loop during ST between the [HS-HS] and [HS-LS] states, (b) that the [HS-LS] state is of the localized type (not 1:1 [HS-HS]:[LS-LS]), and (c) that rapidly freezing the sample in liquid nitrogen can trap it in a metastable [HS-HS] state (reported before for mononuclear complexes<sup>24</sup> and coordination polymers,<sup>25</sup> but seldom for discrete polynuclear complexes<sup>13</sup>). At 293 K, the Mössbauer spectrum of **1** is typical of HS iron(II) centers (Figure S16, Table S9). On cooling slowly to 200 K, **1** remains [HS-HS], with just a slight increase in isomer shift (due to the second-order Doppler shift<sup>26</sup>) and quadrupole splitting (commonly observed in SCO compounds<sup>19c</sup>) (Figures S16–S19). On further slow cooling, to 160 K, a small amount of the pure [HS-HS] state remains (weak shoulders on the outer edges of the main HS quadrupole doublet), however the bulk of the sample has undergone SCO to the localized [HS-LS] state. While the new, intense HS quadrupole doublet has a similar isomer shift to before, the quadrupole splitting is narrower due to the HS iron(II) being affected by the neighboring iron(II) being LS rather than HS (as first observed without applying a magnetic field in the analogous PMAT complex<sup>19b</sup>). This is because of the highly constrained nature of dinuclear complexes of PMRT ligands (Figure 4), a feature which allows us to readily identify the nature of the “[HS-LS]” species (as being localized). When **1** is slowly warmed back up to 200 K, a spectrum consistent with predominantly [HS-LS], and completely different from the [HS-HS] spectrum observed at 200 K on cooling, is seen (Figure S16), consistent with hysteresis.

In conclusion, **1** undergoes abrupt SCO between [HS-HS] and localized [HS-LS] with a record equaling thermal hysteresis loop width for a dinuclear SCO-active complex. Close examination of this loop has clearly demonstrated the critical importance of scan rate on the width of a thermal hysteresis loop and revealed unique scan rate dependence whereby on slowing the scan rate only

the cooling branch narrows, while the heating branch remains unaffected. Future reports of thermal hysteresis should include scan rate details, ideally alongside figures showing the results of scan rate dependence studies, with a view to future reviews being able to include a well-illustrated and referenced section covering this important aspect of hysteretic SCO.

## ■ ASSOCIATED CONTENT

### ■ Supporting Information

Experimental details, literature survey of scan rate information on studies reporting wide hysteresis loops, additional crystallographic, powder XRD, magnetochemistry, Mössbauer and DSC details, fitting of data by Sorai and Seki model and by Slichter and Drickamer model. This material is available free of charge via the Internet at <http://pubs.acs.org>.

## ■ AUTHOR INFORMATION

### Corresponding Author

[sbrooker@chemistry.otago.ac.nz](mailto:sbrooker@chemistry.otago.ac.nz)

### Notes

The authors declare no competing financial interest.

## ■ ACKNOWLEDGMENTS

We thank the University of Otago and the Marsden Fund (RSNZ) for supporting this research, the MacDiarmid Institute for the Mössbauer spectrometer and magnetometers and Dr. S. Chong (IRL) for his help, Assoc. Prof. S. Moratti, I. Stewart, and R. G. Miller (Otago) for their help with the DSC.

## ■ REFERENCES

- Gütlich, P.; Goodwin, H. A. *Top. Curr. Chem.* **2004**, *233*, 1.
- (a) Kahn, O.; Martinez, C. J. *Science* **1998**, *279*, 44. (b) Létard, J.-F.; Guionneau, P.; Goux-Capes, L. *Top. Curr. Chem.* **2004**, *234*, 221. (c) Murray, K. S.; Kepert, C. J. *Top. Curr. Chem.* **2004**, *233*, 195. (d) Brooker, S.; Kitchen, J. A. *Dalton Trans.* **2009**, 7331. (e) Bousseksou, A.; Molnár, G.; Salmon, L.; Nicolazzi, W. *Chem. Soc. Rev.* **2011**, *40*, 3313.
- Halcrow, M. A. *Chem. Soc. Rev.* **2011**, *40*, 4119.
- Buchen, T.; Gütlich, P.; Sugiyarto, K. H.; Goodwin, H. A. *Chem. Eur. J.* **1996**, *9*, 1134.
- Hayami, S.; Kato, K.; Komatsu, Y.; Fuyuhiko, A.; Ohba, M. *Dalton Trans.* **2011**, *40*, 2167.
- (a) Nakamoto, T.; Bhattacharjee, A.; Sorai, M. *Bull. Chem. Soc. Jpn.* **2004**, *77*, 921. (b) Sorai, M.; Ensling, J.; Hasselbach, K. M.; Gütlich, P. *Chem. Phys.* **1977**, *20*, 197.
- Ksenofontov, V.; Levchenko, G.; Spiering, H.; Gütlich, P.; Létard, J. F.; Bouhedja, Y.; Kahn, O. *Chem. Phys. Lett.* **1998**, *294*, 545.
- (a) Müller, B. R.; Leibel, G.; Jäger, E.-G. *Chem. Phys. Lett.* **2000**, *319*, 368. (b) Weber, B.; Bauer, W.; Obel, J. *Angew. Chem., Int. Ed.* **2008**, *47*, 10098. (c) Weber, B.; Bauer, W.; Pfaffeneder, T.; Dirl, M. M.; Naik, A. D.; Rotaru, A.; Garcia, Y. *Eur. J. Inorg. Chem.* **2011**, 3193.
- Muñoz-Lara, F. J.; Gaspar, A. B.; Aravena, D.; Ruiz, E.; Muñoz, M. C.; Ohba, M.; Ohtani, R.; Kitagawa, S.; Real, J. A. *Chem. Commun.* **2012**, *48*, 4686.
- (a) Leita, B. A.; Moubaraki, B.; Murray, K. S.; Smith, J. P.; Cashion, J. D. *Chem. Commun.* **2004**, 156. (b) Nakano, K.; Suemura, N.; Kawata, S.; Fuyuhiko, A.; Yagi, T.; Nasu, S.; Morimoto, S.; Kaizaki, S. *Dalton Trans.* **2004**, 982.
- Nakano, K.; Kawata, S.; Yoneda, K.; Fuyuhiko, A.; Yagi, T.; Nasu, S.; Morimoto, S.; Kaizaki, S. *Chem. Commun.* **2004**, 2892.
- (a) Klingele, M. H.; Moubaraki, B.; Cashion, J. D.; Murray, K. S.; Brooker, S. *Chem. Commun.* **2005**, 987. (b) Amoores, J. J. M.; Kepert, C. J.; Cashion, J. D.; Moubaraki, B.; Neville, S. M.; Murray, K. S. *Chem. Eur. J.* **2006**, *12*, 8220.
- (13) Olguín, J.; Brooker, S. In *Spin-Crossover Materials: Properties and Applications*; Halcrow, M. A., Ed.; John Wiley & Sons, Ltd.: Chichester, UK, 2013; p 77; ISBN: 9781119998679.
- (14) (a) Ksenofontov, V.; Gaspar, A. B.; Niel, V.; Reiman, S.; Real, J. A.; Gütlich, P. *Chem. Eur. J.* **2004**, *10*, 1291. (b) Min, K. S.; Swierczek, K.; DiPasquale, A. G.; Rheingold, A. L.; Reiff, W. M.; Arif, A. M.; Miller, J. S. *Chem. Commun.* **2008**, 317. (c) Schneider, C. J.; Moubaraki, B.; Cashion, J. D.; Turner, D. R.; Leita, B. A.; Batten, S. R.; Murray, K. S. *Dalton Trans.* **2011**, *40*, 6939. (d) Sunatsuki, Y.; Kawamoto, R.; Fujita, K.; Maruyama, H.; Suzuki, T.; Ishida, H.; Kojima, M.; Iijima, S.; Matsumoto, N. *Inorg. Chem.* **2009**, *48*, 8784.
- (15) Weber, B.; Kaps, E. S.; Obel, J.; Achterhold, K.; Parak, F. G. *Inorg. Chem.* **2008**, *47*, 10779.
- (16) While scan rate is not explicitly discussed, the discussion of the basis of hysteresis and of both the Seki–Sorai and Slichter–Drickamer models in the following, in particular Figures 4.8 and 4.9, is helpful: Kahn, O. *Molecular Magnetism*; VCH Publishers Inc.: New York, 1993; pp 59–69.
- (17) Mathonière, C. Photo-induced electron transfer in cyanido molecular complexes (included slides showing a scan rate study of a hysteretic SCO event). Presented at the 13th International Conference on Molecule-based Magnets (ICMM), Orlando, FL, Oct 9–11, 2012.
- (18) (a) Seredyuk, M.; Gaspar, A. B.; Ksenofontov, V.; Galyametdinov, Y.; Kusz, J.; Gütlich, P. *Adv. Funct. Mater.* **2008**, *18*, 2089. (b) Gütlich, P.; Grunert, C. M.; Goodwin, H. A.; Carbonera, C.; Letard, J.-F.; Kusz, J. J. *Phys. Chem. B* **2007**, *111*, 6738. (c) Roubeau, O.; Castro, M.; Burriel, R.; Haasnoot, J. G.; Reedijk, J. *J. Phys. Chem. B* **2011**, *115*, 3003. (d) Rodríguez-Velamazán, J. A.; Castro, M.; Palacios, E.; Burriel, R.; Kitazawa, T.; Kawasaki, T. *J. Phys. Chem. B* **2007**, *111*, 1256. (e) Létard, J.-F.; Asthana, S.; Shepherd, H. J.; Guionneau, P.; Goeta, A. E.; Suemura, N.; Ishikawa, R.; Kaizaki, S. *Chem. Eur. J.* **2012**, *18*, 5924. (f) Seredyuk, M.; Muñoz, M. C.; Castro, M.; Romero-Morcillo, T.; Gaspar, A. B.; Real, J. A. *Chem. Eur. J.* **2013**, *19*, 6591.
- (19) (a) Bhattacharjee, A.; Ksenofontov, V.; Kitchen, J. A.; White, N. G.; Brooker, S.; Gütlich, P. *Appl. Phys. Lett.* **2008**, *92*, 174104. (b) Grunert, C. M.; Reiman, S.; Spiering, H.; Kitchen, J. A.; Brooker, S.; Gütlich, P. *Angew. Chem., Int. Ed.* **2008**, *47*, 2997. (c) Kitchen, J. A.; White, N. G.; Jameson, G. N. L.; Tallon, J. L.; Brooker, S. *Inorg. Chem.* **2011**, *50*, 4586. (d) Kitchen, J. A.; Olguín, J.; Kulmaczewski, R.; White, N. G.; Milway, V. A.; Jameson, G. N. L.; Tallon, J. L.; Brooker, S. *Inorg. Chem.* **2013**, *52*, 11185.
- (20) Real, J. A.; Bolvin, H.; Bousseksou, A.; Dworkin, A.; Kahn, O.; Varret, F.; Zarembowitch, J. *J. Am. Chem. Soc.* **1992**, *114*, 4650.
- (21) Sorai, M. *Top. Curr. Chem.* **2004**, *235*, 153.
- (22) Sorai, M.; Seki, S. *J. Phys. Chem. Solids* **1974**, *35*, 555.
- (23) Slichter, C. P.; Drickamer, H. G. *J. Chem. Phys.* **1972**, *56*, 2142.
- (24) (a) Marchivie, M.; Guionneau, P.; Létard, J. F.; Chasseau, D.; Howard, J. A. K. *J. Phys. Chem. Solids* **2004**, *65*, 17. (b) Money, V. A.; Carbonera, C.; Elhaik, J.; Halcrow, M. A.; Howard, J. A. K.; Létard, J.-F. *Chem. Eur. J.* **2007**, *2007*, 5503. (c) Sheu, C.-F.; Chen, S.-M.; Wang, S.-C.; Lee, G.-H.; Liu, Y.-H.; Wang, Y. *Chem. Commun.* **2009**, 7512. (d) Craig, G. A.; Costa, J. S.; Roubeau, O.; Teat, S. J.; Aromi, G. *Chem. Eur. J.* **2011**, *17*, 3120.
- (25) (a) Ikuta, Y.; Ooidemizu, M.; Yamahata, Y.; Yamada, M.; Osa, S.; Matsumoto, N.; Iijima, S.; Sunatsuki, Y.; Kojima, M.; Dahan, F.; Tuchagues, J.-P. *Inorg. Chem.* **2003**, *42*, 7001. (b) Sunatsuki, Y.; Ikuta, Y.; Matsumoto, N.; Ohta, H.; Kojima, M.; Iijima, S.; Hayami, S.; Maeda, Y.; Kaizaki, S.; Dahan, F.; Tuchagues, J.-P. *Angew. Chem., Int. Ed.* **2003**, *42*, 1614. (c) Yamada, M.; Fukumoto, E.; Ooidemizu, M.; Bréfuel, N.; Matsumoto, N.; Iijima, S.; Kojima, M.; Re, N.; Dahan, F.; Tuchagues, J.-P. *Inorg. Chem.* **2005**, *44*, 6967. (d) Jameson, G. N. L.; Werner, F.; Bartel, M.; Absmeier, A.; Reissner, M.; Kitchen, J. A.; Brooker, S.; Caneschi, A.; Carbonera, C.; Létard, J.-F.; Linert, W. *Eur. J. Inorg. Chem.* **2009**, *26*, 3948.
- (26) (a) Greenwood, N. N.; Gibb, T. C. *Mössbauer Spectroscopy*; Chapman and Hall Ltd.: London, 1971. (b) Gütlich, P.; Bill, E.; Trautwein, A. X. *Mössbauer Spectroscopy and Transition Metal Chemistry*; Springer-Verlag: Berlin/Heidelberg, 2011.